AGU ADVANCING EARTH AND SPACE SCIENCES

Geophysical Research Letters®

Key Points:
- Glacial isostatic adjustment (GIA) is the primary control on slope change for the Red River (ND, USA and MB, Canada) since it began to flow 8.5 ka
- Slope change caused by GIA significantly correlates with river cutoff frequency, a proxy for lateral migration rate
- We infer that slope change modulates the magnitude of shear stress on the riverbank, driving changes in lateral migration rate

Author Contributions:
Conceptualization: Samuel T. Kodama, Tamara Pico, Noah J. Finnegan, Mathieu G. A. Lapôtre, Jane K. Willenbring
Data curation: Samuel T. Kodama
Formal analysis: Samuel T. Kodama
Funding acquisition: Tamara Pico
Investigation: Samuel T. Kodama
Methodology: Samuel T. Kodama, Tamara Pico, Noah J. Finnegan
Project Administration: Tamara Pico
Resources: Tamara Pico
Software: Tamara Pico

Glacial Isostatic Adjustment Modulates Lateral Migration Rate and Morphology of the Red River (North Dakota, USA and Manitoba, Canada)

Samuel T. Kodama[1] [ID], **Tamara Pico[1]** [ID], **Noah J. Finnegan[1]** [ID], **Mathieu G. A. Lapôtre[2]**, and **Jane K. Willenbring[2]** [ID]

[1]Earth and Planetary Sciences, University of California-Santa Cruz, Santa Cruz, CA, USA, [2]Earth and Planetary Sciences, Stanford University, Stanford, CA, USA

Abstract The lateral migration of a river meander is driven by erosion on the outer bank and deposition on the inner bank, both of which are affected by shear stress (and therefore channel slope) through complex morphodynamic feedbacks. To test the sensitivity of lateral migration to channel slope, we quantify slope change induced by glacial isostatic adjustment along the Red River (North Dakota, USA and Manitoba, Canada) and two of its tributaries over the past 8.5 ka. We demonstrate a statistically significant, positive relationship between normalized cutoff count, which we interpret as a proxy for channel lateral migration rate, and slope change. We interpret this relationship as the signature of slope change modulating the magnitude of shear stress on riverbanks, suggesting that slope changes that occur over thousands of years are recorded in river floodplain morphology.

Plain Language Summary Rivers move through the landscape by eroding river bank material on their outer bank and depositing sediment on their inner bank, a process that forms meander bends. Understanding what factors drive river meandering is important for interpreting how rivers interact with landscapes. One factor that could impact river meandering is river slope. To understand the impact of slope on river meandering we quantify how slope has changed along the Red River (North Dakota, USA and Manitoba, Canada) over the past 8.5 Kyr. Over this time, vertical land movement substantially reduced the slope of the river, through the ongoing solid Earth response to the retreat of massive North American ice sheets in a process known as glacial isostatic adjustment (GIA). We find that change in slope, induced by GIA, positively correlates with river migration rate along the Red River, suggesting that slope plays an important role in determining the pace of river meandering.

1. Introduction

Meandering rivers have shaped Earth's landscapes for eons (Ielpi et al., 2022), eroding floodplain sediment as they laterally migrate and depositing new material as point bars. The process of meandering is therefore fundamental to the formation of floodplains. The lateral migration rate of a meander is driven by a combination of the balance of shear stress relative to bank strength, causing erosion on the concave outer bank, and deposition on the convex inner bank (Constantine et al., 2014; Ielpi & Lapôtre, 2020; Parker et al., 2011), both of which are affected by channel bed slope through complex morphodynamic feedbacks with flow and sediment transport.

Channel bed slope is a dominant control on river evolution, and meandering would respond differently to perturbations in slope depending on whether meander migration is a detachment-limited or transport-limited process. In detachment-limited rivers, the slope of a river's long profile will directly impact bed and bank shear stress and thus rates of meander migration. In contrast, for a transport-limited river, meander migration rate will depend on the local divergence of the sediment flux, which depends on the curvature of a river's long profile (Whipple & Tucker, 2002). In order to explore the role of slope in lateral migration rates for either detachment- or transport-limited rivers, the magnitude and timescale of slope change of the river must first be quantified.

The low-lying Red River (gradient = $5–10 \times 10^{-5}$ m/m) flows northwards from North Dakota, USA to Lake Winnipeg, Canada (Figures 1a and 1b), and is an ideal natural experiment for understanding the controls on meandering rates because the dominant control on slope change since the river's formation is solid Earth deformation in response to ice sheet unloading, known as glacial isostatic adjustment (GIA). As the North American

ice sheets retreated during the last deglaciation, the unloading of these ice sheets caused tens of meters of uplift and subsidence along the profile of the Red River (Figures 1a, 1b, and 2a). Proglacial lakes formed along the periphery of the receding ice sheets (Austermann et al., 2022), including Glacial Lake Agassiz (shaded gray; Figure 1b). The Red River began flowing northward through Glacial Lake Agassiz paleolacustrine sediment at ~8.5 ka when the proglacial lake drained (Teller & Leverington, 2004).

Previous studies speculated about the relationship between GIA and channel lateral migration direction and rate in Canada, however these connections have not been quantitatively explored (Brooks, 2003; Nanson, 1980). More recently, GIA has been shown to impact landscape evolution by diverting channels, changing drainage area, and impacting sediment transport capacity (Pico et al., 2018, 2022; Pico, Mitrovica, et al., 2019; Whitehouse et al., 2007; Wickert, 2016; Wickert et al., 2019). If slope exerts an important control on river meandering, then GIA-induced tilting along the Red River may have modulated lateral migration rates through time and space.

Here we quantify the change in slope along the Red River since 8.5 ka due to GIA, and test if spatial trends in slope change correlate to geomorphic evidence for varying migration rates. Specifically, we compare modeled slope change to a record of cutoff occurrence, a proxy for lateral migration rate (Ielpi et al., 2023), and assess the statistical significance of their relationship by performing a Monte Carlo ensemble of M-estimator linear regressions. To generalize our findings, we also consider two additional tributary river systems in this region, the Assiniboine and Red Lake Rivers. Altogether, our analysis provides a mechanistic framework to interpret the relationship between GIA-driven slope change and lateral migration rate within these river systems.

2. Results

2.1. Glacial Isostatic Adjustment-Induced Slope Change on the Red River

To quantify slope change, we modeled GIA along the modern Red River profile since 8.5 ka, when the river first formed (Teller & Leverington, 2004). Our simulations are based on the sea level theory and pseudospectral algorithm described by Kendall et al. (2005) with a spherical harmonic truncation at degree and order 256. This treatment includes the impact of load-induced Earth rotation changes on sea level (Milne & Mitrovica, 1998), evolving shorelines, and the migration of grounded, marine-based ice (Johnston, 1993; Kendall et al., 2005; Lambeck et al., 2003; Milne et al., 1999). Our GIA simulations require two inputs: (a) an Earth structure model with a depth-varying viscosity of the mantle along with elastic lithospheric thickness; and (b) the space-time geometry of ice sheet history. We adopted the deglacial ice history ICE-6G and its corresponding Earth model VM5a (Peltier et al., 2015). We later explore the sensitivity of slope change to variations in ice history and Earth models (Table S1 in Supporting Information S1). Our simulations predict that the upstream reaches of the Red River subsided up to 22 m from 8.5 ka to present, whereas the downstream reaches uplifted by up to 20 m over the same period (Figures 1a, 1b, and 2a, blue line).

To calculate slope, we first applied a 10 km window smoothing filter to the modern riverbed elevation, extracted from North Dakota Geological Survey and Natural Resources Canada Light Detection and Ranging (LiDAR) datasets (black; Figure 2a). We then subtract our modeled GIA-induced topographic change to reconstruct the paleotopography at 8.5 ka (purple; Figure 2a). Next, we determine the corresponding change in slope due to GIA from 8.5 ka to present by dividing the river into reaches, where the length of the reach is scaled by channel width to account for the effects of upstream channel area ($n = 21$, length = 25–100 km; Supporting Information S1; Schumm, 1968), and calculate the slope of each river reach at 8.5 ka and at present. From 8.5 ka to present, we found that GIA reduced the slope in upstream reaches by 5%–20%, whereas in downstream reaches the slope was reduced by 40%–60% (Figure 2b).

2.2. Cutoffs as a Proxy for Channel Lateral Migration Rate Changes Since 8.5 ka

We quantify lateral migration rate, using meander cutoffs as a proxy, to compare to slope change along the Red River (Supporting Information S1). Meander cutoffs form when meanders laterally migrate into upstream or downstream reaches of the same river. Therefore, the amount of time needed to produce a cutoff is proportional to lateral migration rate (Ielpi et al., 2023). Our quantification of cutoff occurrence is consistent with variability in cutoffs that have previously been documented along the Red River (Phillips, 2020). To further understand the nature of Red River meandering, we explored whether the Red River is incising vertically across
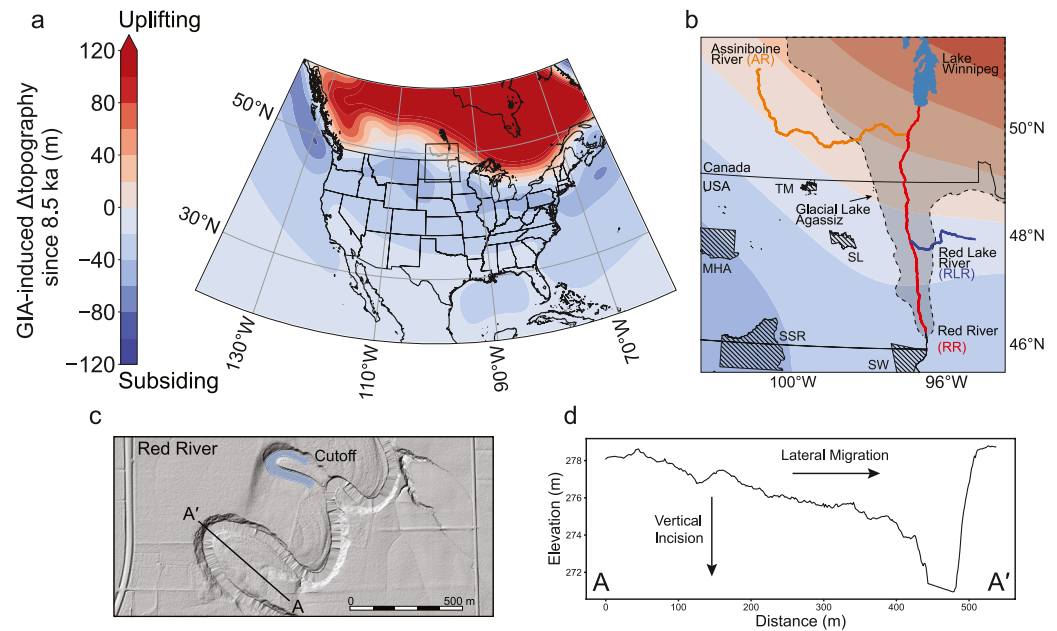
Figure 1. (a) Change in topography due to glacial isostatic adjustment since 8.5 ka. Gray lines show Red River Valley rivers. Black box shows extent of panel (b). (b) Inset within Red River Valley area, including Glacial Lake Agassiz extent at ~10.6 ka (shaded gray; Teller et al., 2004). Crosshatches represent MHA, Mandan, Hidatsa, and Arikara Nations; SSR, Standing Rock Sioux Tribe; SWO, Sisseton Wahpeton Oyate Nation; SL, Spirit Lake Nation; TMB, Turtle Mountain Band of Chippewa (c) LiDAR-derived hillshade of a section of the Red River. (d) Cross section view of a representative incising meander scroll from transect A–A′ in panel (c).

the channel during lateral migration. We measured channel cross-sectional elevation profiles through meander scrolls (Figure 1c and Figure S1 in Supporting Information S1), revealing substantial vertical incision in addition to lateral migration, which is supported by limited floodplain stratigraphy (Brooks, 2003).

Overall, faster channel lateral migration should result in higher cutoff frequency. Since all reaches of the Red River have flowed for the same duration (8.5 ka to present), reaches that have faster time-averaged migration rates are thus expected to contain more cutoffs. We normalized the number of cutoffs (C) to the number of meanders (M) within a given reach and define a normalized cutoff count ($\frac{C}{M}$) as the proportion of meanders that have reached cutoff. Two of the analyzed reaches contain urban development that altered the floodplain, which would artificially reduce our normalized cutoff count, and so we chose to exclude them from our analysis (Figure S2 in Supporting Information S1). We found a higher normalized cutoff count ($\frac{C}{M}$) upstream (0–450 km; Figure 2c) compared to downstream (450–850 km, Figure 2c) reaches. The decreasing trend in normalized cutoff count downstream parallels the increasing magnitude of slope reduction caused by GIA (Figures 2b and 2c).

2.3. Statistical Relationship Between $\Delta \text{slope}_{8.5-0\text{ka}}$ and $\frac{C}{M}$ for the Red River

We next assessed whether the observed correlation between GIA-induced slope change and normalized cutoff count ($\frac{C}{M}$) has a statistically significant relationship. First, we quantified the uncertainty on our GIA-induced slope change by performing 11 GIA simulations that included three ice histories and five Earth structures (Table S1 in the Supporting Information S1; Lambeck et al., 2017 for LW-6; Peltier et al., 2015 for ICE-6G; Pico et al., 2020 and Pico, Robel, et al., 2019 for GI-36). We then built a maximum likelihood estimator regression model, $Y = \beta X$ where Y is $\log\left(\frac{C}{M}\right)$ and X is $\Delta \text{slope}_{8.5-0\text{ka}}$. We chose $\log\left(\frac{C}{M}\right)$ as our Y variable because the distribution of $\frac{C}{M}$ values is skewed toward zero, since it is unphysical for these values to be negative. To create an ensemble of $\Delta \text{slope}_{8.5-0\text{ka}}$ values for our regressions, we used a Monte Carlo method to randomly sample from our predicted values of $\Delta \text{slope}_{8.5-0\text{ka}}$ for each river reach to produce simulated datasets of $\Delta \text{slope}_{8.5-0\text{ka}}$. We then ran 1,000 maximum likelihood (M-estimator) linear regressions, and the ensemble median regression line is shown
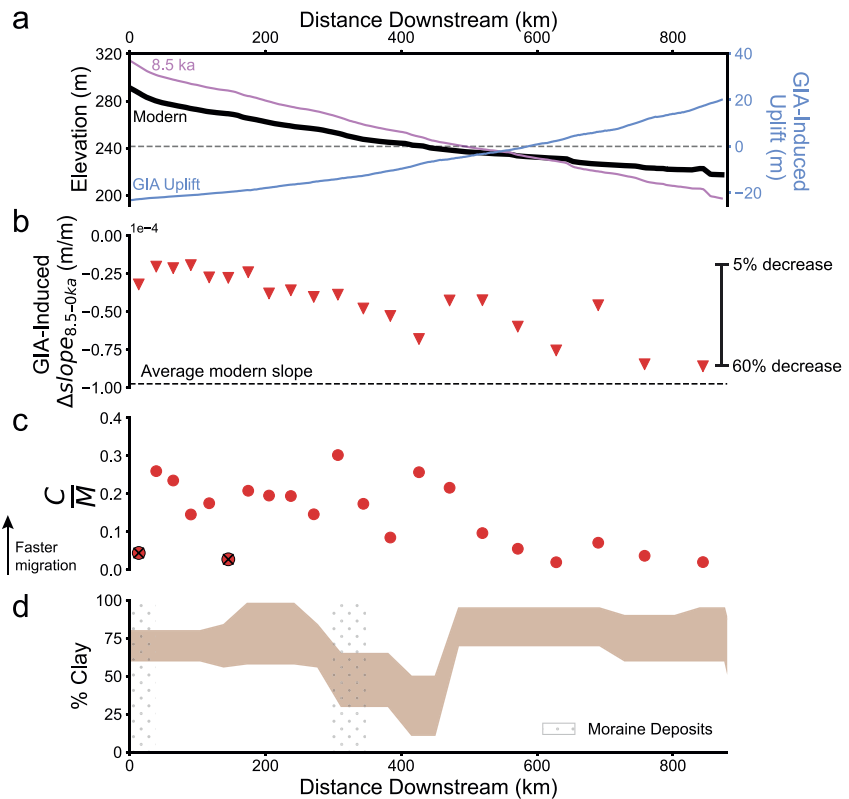
Figure 2. (a) Red River long profile at modern (black), 8.5 ka (light purple), and uplift due to glacial isostatic adjustment (blue). (b) Change in slope from 8.5 ka to present. Dashed line shows the average slope of the modern Red River profile. (c) Normalized cutoff count ($\frac{C}{M}$), computed as the number of cutoffs relative to the number of meander bends per unit length of river. Darker circles with *X* are reaches excluded from statistical analysis due to anthropogenic floodplain reworking (Figure S2 in Supporting Information S1). (d) Percent clay in the banks of the Red River (brown shaded) from Arndt (1997). Moraines are marked with spotted shading (Bush et al., 2003).

for the Red River in Figure 3a (red dashed line). We find that the correlation between $\Delta\text{slope}_{8.5-0ka}$ and $\log(\frac{C}{M})$ is statistically significant (median $p = 4 \times 10^{-4}$). River reaches with the most negative Δ slope contain the least number of cutoffs and therefore record the slowest channel lateral migration rates.
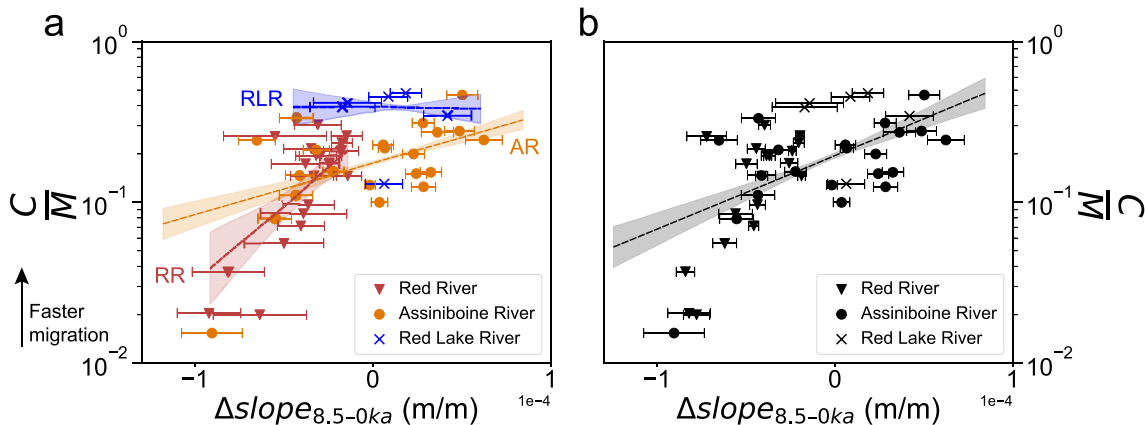
Figure 3. (a) Regressions of $\Delta\text{slope}_{8.5-0ka}$ and log of normalized cutoff count ($\frac{C}{M}$) for the Red River (red), Assiniboine River (orange), and Red Lake River (blue). Shaded regions show 95% confidence interval for Monte Carlo ensemble. Dashed lines show median regression. (b) Regression of $\Delta\text{slope}_{8.5-0ka}$ and log of normalized cutoff count ($\frac{C}{M}$) for all three rivers as a single analysis. Dashed line shows median regression.
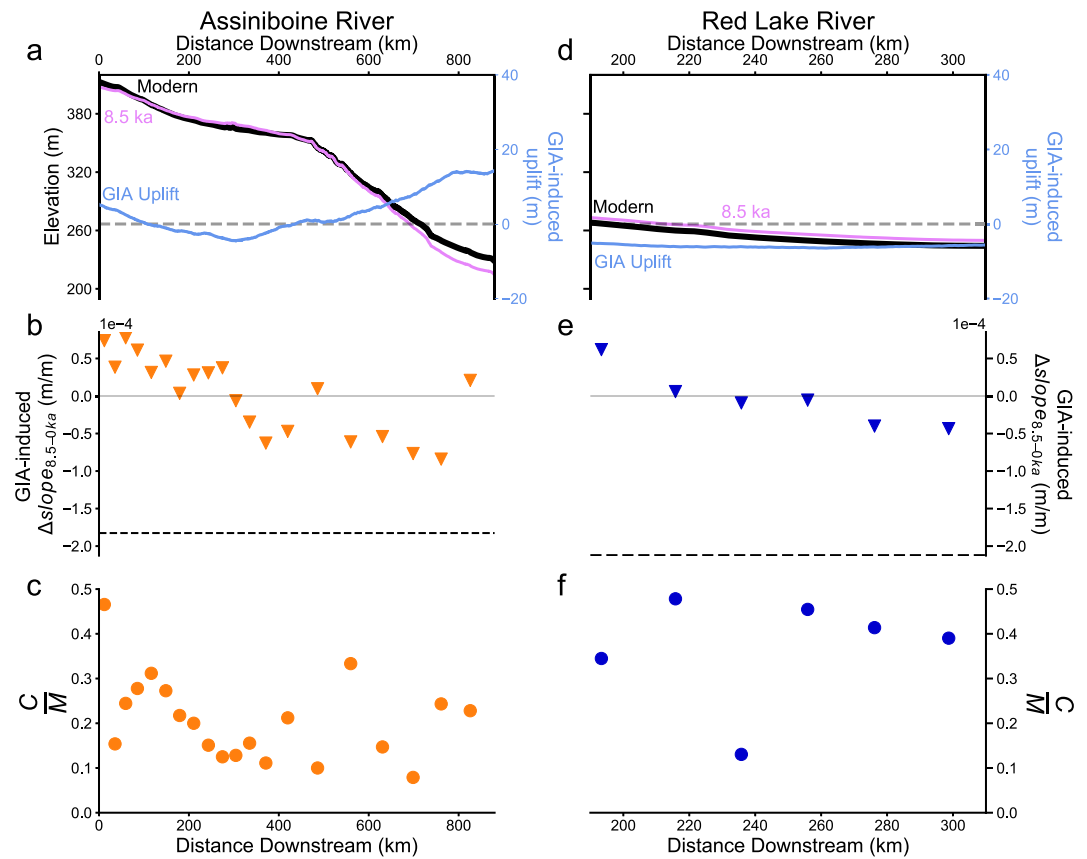
Figure 4. (a) Assiniboine River long profile at modern (black), 8.5 ka (light purple), and uplift due to glacial isostatic adjustment (blue). (b) Change in slope from 8.5 ka to present. The dashed line shows average slope of modern Assiniboine River profile. (c) Normalized cutoff count ($\frac{C}{M}$), computed as the number of cutoffs relative to the number of meander bends per unit length of river. (d)–(f) Same as (a)–(c), but for the Red Lake River.

2.4. Statistical Relationship Between $\Delta slope_{8.5-0ka}$ and $\frac{C}{M}$ for the Assiniboine and Red Lake Rivers

To test whether our finding of a positive relationship between $\Delta slope_{8.5-0ka}$ and normalized cutoff count holds more broadly for the Red River Valley, we expanded our analysis to include the Assiniboine River (mean modern slope $= 1.8 \times 10^{-4}$) and the Red Lake River (mean modern slope $= 2.1 \times 10^{-4}$). These rivers are similar to the Red River with respect to riverbank lithology (Figure S3 in Supporting Information S1), vertical incision (Figure S1 in Supporting Information S1), and base level, as all three rivers drain to Lake Winnipeg (Figure 1b). Due to limitations in available LiDAR coverage, we limit our analysis of the Red Lake River to its downstream reaches (181–310 km). While the Assiniboine River flows through Glacial Lake Agassiz paleolacustrine sediment in the downstream reaches, there are upstream sections that contain glacial till and other alluvial sediment, where the river bank lithology differs from the Red River and the Red Lake River (Figure S3 in Supporting Information S1). A subset of downstream reaches west of Lake Winnipeg underwent multiple avulsions before reaching its modern configuration ca. 2 ka (Bater, 2002; Rannie et al., 1989), however, our results are insensitive to where or not these reaches are included in the analysis (Figure S4 in Supporting Information S1). Interestingly, because the Assiniboine River flows from north to south in its upper reaches, it crosses a GIA gradient that steepens the river by 30%, as opposed to the Red River's decrease in slope. The downstream reaches instead flow west to east, where GIA caused its slope to decrease by up to 40% (Figure 4a). Thus, the Assiniboine River provides an example where GIA caused an increase in slope, opposite to the Red River. In contrast to these two river systems, the Red Lake River experiences little change in slope due to GIA, as it flows parallel to a GIA gradient (less than $\pm8\%$ change in slope; Figure 4d). We use these contrasting examples of GIA-induced slope change to expand our assessment of correlations to normalized cutoff count.

The Assiniboine River contains higher cutoff occurrence upstream (0–300 km), where GIA has increased slopes, and lower cutoff occurrence downstream (300–950 km), where GIA has decreased slopes (Figure 4c). In contrast, the Red Lake River shows no perceptible trend in downstream cutoff occurrence (Figure 4f). We performed the same linear regression ensemble, including uncertainties on slope due to ice history and Earth model (Supporting Information S1), for each of these river systems. For the Assiniboine River we found a positive significant correlation between $\Delta\text{slope}_{8.5-0ka}$ and normalized cutoff count (median $p = 0.006$; Figure 3a), whereas for the Red Lake River we found no correlation between $\Delta\text{slope}_{8.5-0ka}$ and normalized cutoff count (median $p = 0.76$; Figure 3a). We also performed a linear regression ensemble including all three river systems (Red River, Assiniboine River, Red Lake River) and found that a positive correlation still holds (median $p = 0.001$; Figure 3b), despite a noisier data set that spans a range of GIA-induced slope changes and bank lithologies. We assessed the sensitivity of our analysis to parameters in the GIA simulation by building regression models that incorporated GIA simulation output using only the ICE-6G ice history and GIA output using the ICE-6G, LW-6, and GI-36 ice histories. While both models result in a positive correlation with $p < 0.05$ for the Red and Assiniboine Rivers, we find that the ice history impacts the regression coefficient more than the choice of Earth model for all three studied rivers, but especially the Red River (Figure S5 in Supporting Information S1).

3. Discussion

What is the mechanism through which slope change can control lateral migration rate? First, we must understand how the Red River acts geomorphologically. Based on the observed vertical incision along the Red River, and the fact that the Red River flows through cohesive clay-rich, paleolacustrine sediment, we interpret the Red River as a detachment-limited system, which is consistent with other post-glacial rivers systems in the US Midwest such as the Le Sueur River (Gran et al., 2013). In a detachment-limited river channel, bank migration rate (Mr) is related to lateral erosion rate (ϵ) through

$$Mr = I\epsilon \tag{1}$$

where I is an intermittency factor to account for the frequency of discharge events that are sufficient to produce geomorphic change. Lateral erosion rate (ϵ) can be modeled as

$$\epsilon = k(\tau_w - \tau_c) \tag{2}$$

where k is the erodibility of the bank, τ_w is the shear stress applied to the bank, and τ_c is the critical shear stress necessary to erode the bank (Howard & Knutson, 1984). In a river channel, the shear stress induced by flow along the channel boundary is partitioned between the bed and banks (Knight et al., 1984). Such that

$$\tau_w = \tau_b a \tag{3}$$

where τ_b is the bed shear stress and a is a function of a river's aspect ratio (Knight et al., 1984). Bed shear stress, τ_b, can be approximated under steady uniform flow conditions for a gently sloping channel as

$$\tau_b = \rho g h s \tag{4}$$

where ρ is water density, g is gravity, and h is flow depth. We assume here that the meander curvature and aspect ratio of the channel, and therefore the stress partitioning within meander bends, does not change over time. In the case of the Red River, bank lithology, and therefore erodibility (k), is constant through time because the Red River floodplain is homogeneously composed of Glacial Lake Agassiz sediment. Further assuming constant I and channel width-to-depth ratios (a) through time for simplicity, the relative change in Mr caused by change in slope (Δs) through time can be expressed as

$$\frac{Mr_{\text{modern}}}{Mr_0} \propto \frac{1 + \frac{\Delta s}{s_0} - X}{1 - X} \tag{5}$$

in which

$$X = \frac{\tau_c}{a\rho g h s_0} \tag{6}$$

where Δs is the change in slope since 8.5 ka and s_0 is the initial slope at 8.5 ka. Equation 5 shows that an increase in slope should drive an increase in channel lateral migration rate (Mr) and vice versa. In our data set, normalized cutoff count ($\frac{C}{M}$), a proxy for a time-averaged meander rate (average Mr from 8.5 to 0 ka), correlates with reduction in slope along the Red River (Figure 3a). We interpret the observed relationship between change in slope ($\Delta \text{slope}_{8.5-0\text{ka}}$) and normalized cutoff count ($\frac{C}{M}$) as a reflection of changes in time-averaged lateral migration rate in the Red River. Under a reduction in slope, the outer bank is eroded at a slower rate due to a decrease in shear stress, thus leading to slower channel migration. This interpretation is also consistent with a measured decrease in channel lateral migration rate over the past 8.5 ka for two meander scrolls of the Red River located in Manitoba, Canada (Brooks, 2003). We also estimated vertical incision since 8.5 ka (Supporting Information S1) and found that total vertical incision is weakly correlated with change in slope (Figure S6 in Supporting Information S1), which we would expect in a detachment limited system.

In the Assiniboine River, an increase in slope causes Mr to increase due to an increase in outer bank erosion rate, which is consistent with observations that cutoff frequency is higher in river reaches with slope increase (Figure 3a). In contrast, the Red Lake River experiences small changes in slope, which leads to lateral migration rates (Mr) not appreciably changing through time or across river reaches (Figure 3a).

We also considered other variables that may have influenced patterns of cutoff frequencies such as bank lithology, climate change, and base level changes. A previous study showed that clay content, and therefore cohesion, is high along the Red River Valley, with clay content varying from 11% to 98% (Arndt, 1977). We found a weak, negative relationship between percent clay and normalized cutoff count; however, this relationship was not statistically significant (median $p = 0.11$; Figure S7 in Supporting Information S1). The Red River also flows through two moraines (Figure 2d; Text S3 in Supporting Information S1), the Comstock Moraine (~0–40 km downstream) and the Edinburgh Moraine (~300–350 km downstream), (Bush et al., 2003; Harris et al., 1974), nevertheless, these moraines are narrow in extent and cannot explain the long-profile variability in cutoff frequency.

Throughout the Holocene, the central North American midwest experienced changes in climate that affected precipitation and aridity over the Red River Valley until 4 ka, when conditions became more humid (Bartlein et al., 1984; Grimm et al., 2001; Valero-Garcés et al., 1997; Wanner et al., 2008). Changes in aridity and precipitation could affect channel lateral migration rate through changes in river discharge, however these regional Holocene climate trends would influence aridity and precipitation similarly across each of the three river systems we examined. An increase in mid- to late- Holocene humidity led to a 10 m base level rise of Lake Winnipeg from 4 ka to present (Lewis et al., 2001). Bathymetric models of Lake Winnipeg show shallow lake bed slopes (~10^{-4}) within a factor of 2–6 of the modern Red River slope (Rudolfsen et al., 2021). Due to the similarity in slope between the lake and river beds, any geomorphic response by the Red River to reestablish equilibrium flow would likely be minimal. Based on calculating backwater length as the ratio of flow depth (4 m, Kimiaghalam et al., 2015) to bed slope (2×10^{-4}), we estimate a backwater length of ~20 km, which is not sufficiently long to cause decreases in normalized cutoff count hundreds of kilometers upstream from the river outlet. We conclude that bank lithology, climate change, and base level changes cannot fully explain the observed trend in lateral migration rate changes from 8.5 ka to the present, and slope likely played a more important role in these river systems.

While our proposed mechanistic framework of slope change (Δslope) modulating bank shear stress (τ_w) applies to detachment-limited systems, the role of slope within a transport-limited system might differ. Within a transport-limited system, divergence of sediment transport is proportional to the gradient in slope (Exner, 1920, 1925; Ferrer-Boix et al., 2016), and assuming steady uniform flow, long profile river bed curvature controls patterns of erosion and deposition. Therefore, changes in long-profile curvature caused by GIA uplift or subsidence may have implications for aggradation and degradation patterns in transport-limited rivers that could similarly impact channel lateral migration rate.

4. Conclusion

We quantified slope change due to GIA along the Red River from 8.5 ka to present day, and, based on an analysis of cutoff frequency, found that reaches with a greater reduction in slope correlate with slower time-averaged lateral migration rates. We expanded our analysis to two other tributary river systems and showed a statistically significant positive relationship between slope change due to GIA and normalized

cutoff count, which we used as a proxy for channel lateral migration rate. This relationship holds in all three river systems regardless of sign (negative or positive) of the GIA-induced slope change. We infer that slope drives changes in lateral migration rate for these detachment-limited systems, which we interpret to result from slope change modulating the magnitude of shear stress on riverbanks. This result demonstrates that rivers can respond to changes in slope that occur over thousands of years, suggesting that rivers could serve as archives for crustal deformation occurring over the ice age. Geomorphic records of river evolution on glacial–interglacial timescales provide a unique opportunity to quantify and isolate slope change of a river, and therefore may play a key role in improving our understanding of interactions between landscapes and the solid Earth.

Data Availability Statement

The LiDAR data used to construct modern river bed profiles is from the North Dakota Department Water Resources MapService (https://lidar.dwr.nd.gov/) and Government of Canada High Resolution Digital Elevation Model (HRDEM)—CanElevation Series (https://open.canada.ca/data/en/dataset/957782bf-847c-4644-a757-e383c0057995). Output sea level fields, river centerline shapefiles, locations of cutoffs and meanders, and bounds of river reaches can be found on Zenodo (https://doi.org/10.5281/zenodo.7734810).

References

Arndt, B. M. (1977). *Stratigraphy of offshore sediment Lake Agassiz-North Dakota* (p. 60). North Dakota Geological Survey.

Austermann, J., Wickert, A. D., Pico, T., Kingslake, J., Callaghan, K. L., & Creel, R. C. (2022). Glacial isostatic adjustment shapes proglacial lakes over glacial cycles. *Geophysical Research Letters*, *50*, e2022GL101191. https://doi.org/10.1029/2022GL101191

Bartlein, P. J., Webb, T., & Fleri, E. (1984). Holocene climatic change in the northern Midwest: Pollen-derived estimates. *Quaternary Research*, *22*(3), 361–374. https://doi.org/10.1016/0033-5894(84)90029-2

Bater, C. W. (2002). Meander migration rates and age of the lower Assiniboine River. *Prairie Perspectives: Geographical Essays*, *5*(Rannie 1990), 42–55.

Brooks, G. R. (2003). Holocene lateral channel migration and incision of the Red River, Manitoba, Canada. *Geomorphology*, *54*(3–4), 197–215. https://doi.org/10.1016/S0169-555X(02)00356-2

Bush, D. S., Pennell, J. N., & Fullerton, C. A. (2003). *Surficial deposits and materials in the eastern and central United States (east of 102 degrees west longitude)*. USGS. https://doi.org/10.3133/i2789

Constantine, J. A., Dunne, T., Ahmed, J., Legleiter, C., & Lazarus, E. D. (2014). Sediment supply as a driver of river meandering and floodplain evolution in the Amazon Basin. *Nature Geoscience*, *7*(12), 899–903. https://doi.org/10.1038/ngeo2282

Exner, F. M. (1920). *Zur physik der dünen*. Hölder.

Exner, F. M. (1925). *Über die Wechselwirkung zwischen Wasser und Geschiebe in Flüssen: Gedr. mit Unterstützg aus d. Jerome u. Margaret Stonborough-Fonds*. Hölder-Pichler-Tempsky, A.-G.

Ferrer-Boix, C., Chartrand, S. M., Hassan, M. A., Martín-Vide, J. P., & Parker, G. (2016). On how spatial variations of channel width influence river profile curvature. *Geophysical Research Letters*, *43*(12), 6313–6323. https://doi.org/10.1002/2016GL069824

Gran, K. B., Finnegan, N., Johnson, A. L., Belmont, P., Wittkop, C., & Rittenour, T. (2013). Landscape evolution, valley excavation, and terrace development following abrupt postglacial base-level fall. *Geological Society of America Bulletin*, *125*(11–12), 1851–1864. https://doi.org/10.1130/B30772.1

Grimm, E. C., Lozano-García, S., Behling, H., & Markgraf, V. (2001). Holocene vegetation and climate variability in the Americas. In *Interhemispheric climate linkages*. Elsevier. https://doi.org/10.1016/b978-012472670-3/50022-7

Harris, K. L., Moran, S. R., & Clayton, L. (1974). Late Quaternary stratigraphic nomenclature, Red River Valley, North Dakota and Minnesota. *North Dakota Geological Survey Miscellaneous Series*, *52*(95), 47.

Howard, A. D., & Knutson, T. R. (1984). Sufficient conditions for river meandering: A simulation approach. *Water Resources Research*, *20*(11), 1659–1667. https://doi.org/10.1029/wr020i011p01659

Ielpi, A., & Lapôtre, M. G. A. (2020). A tenfold slowdown in river meander migration driven by plant life. *Nature Geoscience*, *13*(1), 82–86. https://doi.org/10.1038/s41561-019-0491-7

Ielpi, A., Lapôtre, M. G. A., Gibling, M. R., & Boyce, C. K. (2022). The impact of vegetation on meandering rivers. *Nature Reviews Earth and Environment*, *3*(3), 165–178. https://doi.org/10.1038/s43017-021-00249-6

Ielpi, A., Viero, D. P., Lapôtre, M. G. A., Graham, A., Ghinassi, M., & Finotello, A. (2023). How is time distributed in a river meander belt? *Geophysical Research Letters*, *50*, e2022GL101285. https://doi.org/10.1029/2022GL101285

Johnston, P. (1993). The effect of spatially non-uniform water loads on prediction of sea-level change. *Geophysical Journal International*, *114*(3), 615–634. https://doi.org/10.1111/j.1365-246X.1993.tb06992.x

Kendall, R. A., Mitrovica, J. X., & Milne, G. A. (2005). On post-glacial sea level - II. Numerical formulation and comparative results on spherically symmetric models. *Geophysical Journal International*, *161*(3), 679–706. https://doi.org/10.1111/j.1365-246X.2005.02553.x

Kimiaghalam, N., Goharrokhi, M., Clark, S. P., & Ahmari, H. (2015). A comprehensive fluvial geomorphology study of riverbank erosion on the Red River in Winnipeg, Manitoba, Canada. *Journal of Hydrology*, *529*, 1488–1498. https://doi.org/10.1016/j.jhydrol.2015.08.033

Knight, D. W., Demetriou, J. D., & Hamed, M. E. (1984). Boundary shear in smooth rectangular channels. *Journal of Hydraulic Engineering*, *110*(4), 405–422. https://doi.org/10.1061/(asce)0733-9429(1984)110:4(405)

Lambeck, K., Purcell, A., Johnston, P., Nakada, M., & Yokoyama, Y. (2003). Water-load definition in the glacio-hydro-isostatic sea-level equation. *Quaternary Science Reviews*, *22*(2–4), 309–318. https://doi.org/10.1016/S0277-3791(02)00142-7

Lambeck, K., Purcell, A., & Zhao, S. (2017). The North American Late Wisconsin ice sheet and mantle viscosity from glacial rebound analyses. *Quaternary Science Reviews*, *158*, 172–210. https://doi.org/10.1016/j.quascirev.2016.11.033

Lewis, C. F. M., Forbes, D. L., Todd, B. J., Nielsen, E., Thorleifson, L. H., Henderson, P. J., et al. (2001). Uplift-driven expansion delayed by middle Holocene desiccation in Lake Winnipeg, Manitoba, Canada. *Geology*, *29*(8), 743. https://doi.org/10.1130/0091-7613(2001)029<0743:UDEDBM>2.0.CO;2

Milne, G. A., & Mitrovica, J. X. (1998). Postglacial sea-level change on a rotating Earth. *Geophysical Journal International*, *133*(1), 1–19. https://doi.org/10.1046/j.1365-246X.1998.1331455.x

Milne, G. A., Mitrovica, J. X., & Davis, J. L. (1999). Near-field hydro-isostasy: The implementation of a revised sea-level equation. *Geophysical Journal International*, *139*(2), 464–482. https://doi.org/10.1046/j.1365-246X.1999.00971.x

Nanson, G. C. (1980). A regional trend to meander migration. *The Journal of Geology*, *88*(1), 100–108. https://doi.org/10.1086/628477

Parker, G., Shimizu, Y., Wilkerson, G. V., Eke, E. C., Abad, J. D., Lauer, J. W., et al. (2011). A new framework for modeling the migration of meandering rivers. *Earth Surface Processes and Landforms*, *36*(1), 70–86. https://doi.org/10.1002/esp.2113

Peltier, W. R., Argus, D. F., & Drummond, R. (2015). Space geodesy constrains ice age terminal deglaciation: The global ICE-6G_C (VM5a) model. *Journal of Geophysical Research: Solid Earth*, *120*(1), 450–487. https://doi.org/10.1002/2014JB011176

Phillips, Z. R. (2020). Holocene postglacial fluvial processes and landforms in low relief landscapes. ProQuest Dissertations and Theses. North Dakota State University PP. Retrieved from https://www.proquest.com/dissertations-theses/holocene-postglacial-fluvial-processes-landforms/docview/2439292152/se-2?accountid=14523

Pico, T., David, S. R., Larsen, I. J., Mix, A. C., Lehnigk, K., & Lamb, M. P. (2022). Glacial isostatic adjustment directed incision of the Channeled Scabland by Ice Age megafloods. *Proceedings of the National Academy of Sciences of the United States of America*, *119*(8), 1–8. https://doi.org/10.1073/pnas.2109502119

Pico, T., Mitrovica, J. X., Braun, J., & Ferrier, K. L. (2018). Glacial isostatic adjustment deflects the path of the ancestral Hudson River. *Geology*, *46*(7), 591–594. https://doi.org/10.1130/G40221.1

Pico, T., Mitrovica, J. X., & Mix, A. C. (2020). Sea level fingerprinting of the Bering Strait flooding history detects the source of the Younger Dryas climate event. *Science Advances*, *6*(9), eaay2935. https://doi.org/10.1126/sciadv.aay2935

Pico, T., Mitrovica, J. X., Perron, J. T., Ferrier, K. L., & Braun, J. (2019). Influence of glacial isostatic adjustment on river evolution along the U.S. mid-Atlantic coast. *Earth and Planetary Science Letters*, *522*, 176–185. https://doi.org/10.1016/j.epsl.2019.06.026

Pico, T., Robel, A., Powell, E., Mix, A. C., & Mitrovica, J. X. (2019). Leveraging the rapid retreat of the Amundsen Gulf Ice Stream 13,000 years ago to reveal insight into North American deglaciation. *Geophysical Research Letters*, *46*(21), 12101–12107. https://doi.org/10.1029/2019GL084789

Rannie, W. F., Thorleifson, L. H., & Teller, J. T. (1989). Holocene evolution of the Assiniboine River paleochannels and Portage la Prairie alluvial fan. *Canadian Journal of Earth Sciences*, *26*(9), 1834–1841. https://doi.org/10.1139/e89-156

Rudolfsen, T. A., Watkinson, D. A., Charles, C., Kovachik, C., & Enders, E. C. (2021). Developing habitat associations for fishes in Lake Winnipeg by linking large scale bathymetric and substrate data with fish telemetry detections. *Journal of Great Lakes Research*, *47*(3), 635–647. https://doi.org/10.1016/j.jglr.2021.02.002

Schumm, S. A. (1968). Speculations concerning paleohydrologic controls of terrestrial sedimentation. *Geological Society of America Bulletin*, *79*(11), 1573–1588. https://doi.org/10.1130/0016-7606(1968)79[1573:scpcot]2.0.co;2

Teller, J. T., & Leverington, D. W. (2004). Glacial Lake Agassiz: A 5000 yr history of change and its relationship to the $\delta^{18}O$ record of Greenland. *Bulletin of the Geological Society of America*, *116*(5–6), 729–742. https://doi.org/10.1130/B25316.1

Valero-Garcés, B. L., Laird, K. R., Fritz, S. C., Kelts, K., Ito, E., & Grimm, E. C. (1997). Holocene climate in the Northern Great Plains inferred from sediment stratigraphy, stable isotopes, carbonate geochemistry, diatoms, and pollen at Moon Lake, North Dakota. *Quaternary Research*, *48*(3), 359–369. https://doi.org/10.1006/qres.1997.1930

Wanner, H., Beer, J., Bütikofer, J., Crowley, T. J., Cubasch, U., Flückiger, J., et al. (2008). Mid- to Late Holocene climate change: An overview. *Quaternary Science Reviews*, *27*(19–20), 1791–1828. https://doi.org/10.1016/j.quascirev.2008.06.013

Whipple, K. X., & Tucker, G. E. (2002). Implications of sediment-flux-dependent river incision models for landscape evolution. *Journal of Geophysical Research*, *107*(B2), 2039. https://doi.org/10.1029/2000JB000044

Whitehouse, P. L., Allen, M. B., & Milne, G. A. (2007). Glacial isostatic adjustment as a control on coastal processes: An example from the Siberian Arctic. *Geology*, *35*(8), 747–750. https://doi.org/10.1130/G23437A.1

Wickert, A. D. (2016). Reconstruction of North American drainage basins and river discharge since the Last Glacial Maximum. *Earth Surface Dynamics*, *4*(4), 831–869. https://doi.org/10.5194/esurf-4-831-2016

Wickert, A. D., Anderson, R. S., Mitrovica, J. X., Naylor, S., & Carson, E. C. (2019). The Mississippi River records glacial-isostatic deformation of North America. *Science Advances*, *5*(1), 1–8. https://doi.org/10.1126/sciadv.aav2366

References From the Supporting Information

Lane, E. W. (1937). Stable channels in erosible material. *Transactions of the American Society of Civil Engineers*, *102*(1), 123–142. https://doi.org/10.1061/TACEAT.0004841

Last, W., & Teller, J. (2002). Paleolimnology of Lake Manitoba: The lithostratigraphic evidence. *Géographie Physique et Quaternaire*, *56*(2–3), 135–154. https://doi.org/10.7202/009101ar

Wheeler, J. O., Hoffman, P. F., Card, K. D., Davidson, A., Sanford, B. V., Okulitch, A. V., & Roset, W. R. (1996). *Geological map of Canada / Carte Géologique Du Canada*. Natural Resources Canada. https://doi.org/10.4095/208175